



Corrosion Resistance and Surface Protective Performance of Waste Material of *Eucalyptus globulus* for Low Carbon Steel

Rajesh Haldhar¹ · Dwarika Prasad²

Received: 16 November 2019 / Revised: 21 January 2020 / Accepted: 18 February 2020 / Published online: 9 March 2020
© Springer Nature Switzerland AG 2020

Abstract

Eucalyptus globulus (*E. globulus*) leave's extract was tested for corrosion inhibition on the low carbon steel (LCS) in a 0.5 M sulphuric acid solution using weight loss, Tafel and EIS. The state of mixed adsorption with the potentiodynamic polarization effect is shown. *E. globulus* showed the strongest corrosion inhibition of 93.09% at a concentration of 600 mg/L. SEM and AFM are used to verify the formation of a protective layer on the surface of LCS. The adsorption phenomenon was verified using UV–Vis spectroscopic technique, whereas FT-IR confirmed the presence of several functional groups containing heteroatoms. Adsorption of the inhibitory molecules on the LCS surface followed the Langmuir adsorption isotherm. Theoretical studies were conducted to validate the study. All obtained results ensure that *E. globulus* leave's extract can form an effective blocking layer and control the corrosion process.

Keywords LCS · EIS · Polarization · Weight loss · SEM · Theoretical studies · Surface treatment

1 Introduction

Low carbon steel (mild steel) is largely used for making a comprehensive variety of metallic structures and hardware. It is cheap and easily available in the market [1]. In industries when it comes in contact with the different industrial process like acid pickling, then corrosion takes place. The indirect and direct cost including common coatings of corrosion for India is US\$ 26.1 billion or 2.4% and 49.75 billion or 4.5% of GDP [2]. However, in recent times, some synthetic corollary might be shown by the synthetic compounds, which may be pernicious for the environment as well as for the human health are preferred more to be used as corrosion inhibitors [3, 4]. An extensive class of corrosion inhibitors is constituted in natural products. The easy availability and

non-toxicity give the plant extract a meaningful excellency to be used as a prohibition for corrosion [5–7]. The effectiveness of the corrosion process inhibited by plant extract on the LCS surface is established due to the presence of chemical constituents such as flavonoids, polyphenols and polysaccharides [8–11]. Natural products containing functional groups such as NH₂, carbonyl and CHO group are known to have feasible inhibition power [12–16]. Many researchers have already reported different plants as a green corrosion inhibitor for the acidic medium with good inhibition efficiency. Table 1 shows the previously reported green corrosion inhibitors by other researchers [17–32]. Although most of the previously reported green inhibitors showed good inhibition efficiencies, a higher inhibitor concentration was used there; this concern motivated us to conduct this investigation. To the best of author's knowledge, this plant has not been used previously for corrosion inhibition study. Moreover, it provides good inhibition efficiency at low inhibitor concentration.

Eucalyptus globulus is an evergreen tree and generally grows up to 30–55 m (98–180 ft). This tree bears simple, alternate leaves 6–15 cm across. It belongs to the *Myrtaceae* family and known as eucalyptus, bluegum and Tasmanian bluegum. It is commonly found throughout India, Australia, Southern Africa, New Zealand and the western United States. Leaves of *E. globulus* are very easily available in the market. *E.*

Electronic supplementary material The online version of this article (<https://doi.org/10.1007/s40735-020-00340-3>) contains supplementary material, which is available to authorized users.

✉ Dwarika Prasad
dwarika123.maithani@gmail.com

¹ Department of Chemistry, Lovely Professional University, Phagwara 144411, India

² Department of Chemistry, Shri Guru Ram Rai University, Dehradun 248001, India

Table 1 Inhibition efficiencies of previously studied plant extracts

S. No	Inhibitor	Efficiency (%)	Inhibitor concentration (mg/L)
1	<i>Salvia officinalis</i> ¹⁷	96	2500
2	<i>Myristica fragrans</i> ¹⁸	87	500
3	<i>Mangrove tannins</i> ¹⁹	89	6000
4	<i>Jasminum nudiflorum</i> ²⁰	92	1000
5	<i>Lawsonia</i> ²¹	92	1200
6	<i>Dendrocalamus brandisii</i> ²²	90	1000
7	<i>Coffee</i> ²³	83	400
8	<i>Phyllanthus amarus</i> ²⁴	81	4000
9	<i>Black radish</i> ²⁵	92	1000
10	<i>Ginkgo</i> ²⁶	80	100
11	<i>Kola nitida</i> ²⁷	78	1200
12	<i>Radish</i> ²⁸	79	10
13	<i>Acacia concinna</i> ²⁹	92	250
14	<i>Bamboo</i> ³⁰	89	200
15	<i>Lecaniodiscus cupanioides</i> ³¹	90	1000
16	<i>Gum arabic</i> ³²	97	1000

globulus contains eucalyptol, globulisin-A and globulisin-B as major phytochemical compounds [33, 34]. The image of *E. globulus* leaves and its major phytochemical constituents are represented in Fig. 1.

The present investigation is aimed to extract the *E. globulus* leaves and investigate the anti-corrosion properties for LCS in 0.5 M sulphuric acid, based on gravimetric measurements and electrochemical analysis. In addition, surface adsorption of the inhibitor molecules on the surface of LCS has been studied using atomic force microscopy (AFM) and scanning electron microscopy (SEM). For a better and deeper understanding of the adsorption phenomenon, ultraviolet–visible (UV–Vis.), Fourier-transform infrared (FT-IR) and nuclear magnetic resonance (NMR) spectroscopic techniques have been conducted. All the experimental outcomes were correlated with the theoretical data to better understand the adsorption phenomenon. The novelty of our investigation is to replace the existing synthetic inhibitors by natural inhibitors, and the use of the natural waste material as a green corrosion inhibitor makes it more novel and effective. The advances to use the natural extract as a green inhibitor are as follows: (1) Natural products are eco-friendly and non-hazardous to the environment as well as to the human being and (2) they convert waste products to a useful material with negligible production cost.

2 Experimental

2.1 Preparation of the Working Electrode, Inhibitor and Electrolytes

Fresh *E. globulus* leaves were validated by Dr. A. A. Bhat in the Department of Biotechnology, LPU, Punjab (INDIA). The crude material was thoroughly washed under running water followed by sterile distilled water and dried in the shade. They were grinded to convert in powder. The sample was approximately 100 g of the powder that was extracted in a 500-mL round bottom flask with 250 mL of solvent. The filtrate was collected and concentrated using a rotary evaporator under controlled temperature and pressure conditions. The extracts were concentrated to dryness to give a crude residue. Followed by this procedure, around 15% of extract yield with pH value of around 8 was obtained. 1 cm² cubical-shaped LCS specimens were used in weight loss estimations and electrochemical analysis. The LCS specimens were abraded with emery paper of grade 100, 300, 600, 800, 1000 and 1200 then washed with distilled water and acetone, dried again and finally kept in a desiccator until used. The sulphuric acid was diluted to 0.5 M H₂SO₄ to use as the corrosive medium. The test solution with specific concentrations (100–600 mg/L) was obtained by diluting plant extract with 0.5 M sulphuric acid solution. The highest solvency of the *E. globulus* extract in 0.5 M sulphuric acid solution was observed up to 600 mg/L.

2.2 Weight Loss Studies

Weight loss measurements were conducted according to ASTM G 31–72 method at 298 K for 24 h and weighed accurately before and after the tests [35]. All the experiments were performed at a constant temperature (298 K) using PPI Fini X48 digital thermostat. For the precise weighing of the LCS samples, a Shimadzu BL-220H/D455006313 digital electronic weighing balance was used. The LCS specimens were immersed in the 0.5 M sulphuric acid solution containing different inhibitor concentrations at 298 K for 24 h. Weight loss or gravimetric measurement was conducted because that is an extensively used and trust-worthy method.

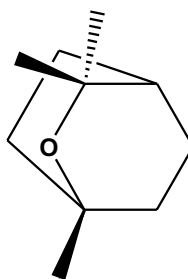
2.3 Electrochemical Studies

Electrochemical impedance spectroscopy (EIS) and potentiodynamic polarization measurements (Tafel) were performed using the CHI760C electrochemical workstation. Experiments were performed at 298 K in 0.5 M sulphuric acid, including various concentrations (100–600 mg/L) of inhibitor. A traditional three-electrode system was used

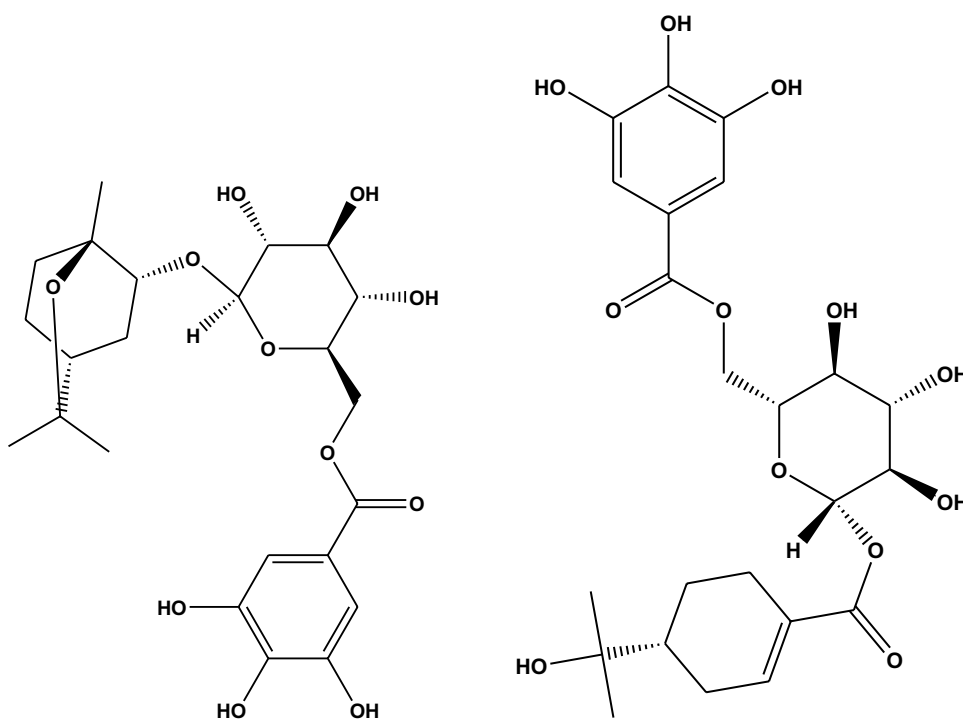
Fig. 1 **a** *E. globulus* leaves, and their main chemical constituents **b** eucalyptol, **c** globulisin-A and **d** globulisin-B



(a)



(b)



(c)

(d)

where LCS with a working area of 1 cm² was used as working electrode. The platinum electrode used as an auxiliary electrode and the saturated calomel electrode (SCE) coupled to a luggin capillary was used as the reference electrode. Before each experiment, the working electrode was immersed in the test solution for 60 min to stabilized

corrosion potential values (E_{corr}). The polarization curves were recorded at ± 250 mV versus SCE with a scanning speed of 1 mV/s. The EIS spectra were scanned with a frequency range of 100 kHz to 0.01 Hz with a signal amplitude perturbation of 0.005 V. Electrochemical

measurements were prepared repeated three times to get reliable values [36].

2.4 UV–Visible Spectroscopy

The UV–Visible spectra of the inhibitor solution before and after immersion of LCS sample for 24 h at 298 K were taken using Shimadzu UV-1800 UV–Visible absorption spectrophotometer at a wavelength of 500–200 nm. Then, they were used to explain the mechanism of inhibition.

2.5 FT-IR and ^1H NMR Spectroscopy

For the identification of the presence of various functional groups, FT-IR analysis has been recorded with the help of Shimadzu 8400S spectrophotometer at a wavenumber range of 500–4000 cm^{-1} . ^1H NMR spectrum has been done to verify the presence of the prime phytochemical constituent in the plant extract. For NMR, Bruker Advance II 400 MHz system was used.

2.6 Surface Investigations

For the surface analysis, scanning electron microscope (SEM-Model: LEO-435 VP) and atomic force microscope (AFM-Model: NT-MDT-INTEGRA) images of pre-treated LCS specimen, LCS in 0.5 M sulphuric acid, without and with the inhibitor extract (600 mg/L) for 24 h at 298 K were taken out.

2.7 Quantum Chemical Calculations

Theoretical studies were carried out to a deeper understanding of the adsorption mechanism. Quantum chemical calculations were used as theoretical studies. It is a well-known fact that the extract of plants has several phytochemical constituents. For the theoretical studies, we followed the presence of three main phytochemical constituents in the plant extract *E. globulus*. Quantum chemical calculations were conducted using density functional theory (DFT) with Hyperchem 8.0 software. Key parameters were obtained from the optimized structures.

3 Results and Discussions

3.1 Gravimetric Measurements and Adsorption Isotherm

Gravimetric measurements were carried out as per ASTM G 31–72 method for 24 h at 298 K with different inhibitor concentrations in 0.5 M H_2SO_4 solution. LCS samples were used as per the ASTM method. These experiments

were repeated three times to achieve more precise results. The elemental composition (wt%) of used LCS samples were Fe = 97.83%, Mn = 0.43%, P = 0.12%, Si = 0.39%, Cu = 0.43%, C = 0.08%, Ni = 0.27% and Cr = 0.45%. Corrosion rate was determined in the absence and presence of inhibitor using the following equation:

$$C_R = \frac{K \times W}{A \times t \times \rho} \quad (1)$$

where W is the weight loss of LCS strip (g), C_R is the corrosion rate (mmy^{-1}), t is the immersion time (h), K is the constant equals to 8.76×10^4 , ρ the density in g cm^{-3} which is 7.86 g cm^{-3} for mild steel according to ASTM G 31–72, and A is the surface area (cm^2) of LCS. The surface area of the LCS can be calculated using the following equation:

$$A = \frac{\pi}{2}(D^2 - d^2) + \pi D + \pi d \quad (2)$$

The inhibition efficiency (IE %) and surface coverage (θ) values were calculated with the help of the following equations:

$$\text{IE}(\%) = \frac{C_{R-C_R^i}}{C_R^0} \times 100 \quad (3)$$

$$\theta = \frac{C_{R-C_R^i}}{C_R^0} \quad (4)$$

where C_R^0 and C_R^i are the corrosion rate of LCS in the absence and presence of inhibitor, respectively. θ is the surface coverage value. In Eq. (2), D and l are the diameters and the thickness of the specimen, respectively, and d is the diameter of the hole for holding.

The results are presented in Table 2. Corrosion rate decreases with the increasing inhibitor concentration. In the absence of inhibitor, the highest corrosion rate (11.33 mmy^{-1}) was observed, while in the presence of inhibitor

Table 2 Corrosive properties of LCS in 0.5 M H_2SO_4 without and at different concentrations of *E. globulus* for 24 h at 298 K

Inhibitor concentration (mg/L)	C_R (mmy^{-1})	Efficiency (IE%)	θ
0	11.33 ± 0.12	–	–
100	2.27 ± 0.17	79.93	0.7993
200	1.83 ± 0.22	83.77	0.8377
300	1.61 ± 0.27	85.78	0.8578
400	1.36 ± 0.32	87.95	0.8795
500	1.15 ± 0.11	89.79	0.8979
600	1.06 ± 0.13	90.63	0.9063

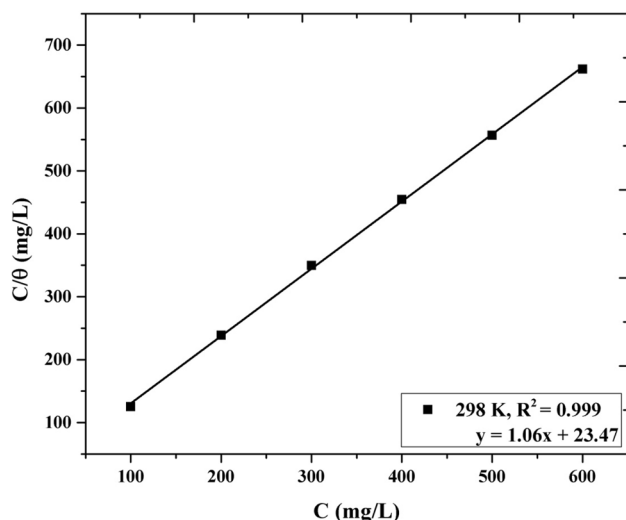


Fig. 2 The Langmuir adsorption isotherm (C/θ vs. C) by measuring the weight loss of the extract *E. globulus* for LCS surface in 0.5 M H_2SO_4 at a temperature of 298 K for 24 h

(600 mg/L), the lowest corrosion rate (1.06 mmy^{-1}) was observed. The highest value of inhibition efficiency achieved is 90.63% at 600 mg/L inhibitor concentration. The Gravimetric measurement values are used to plot the Langmuir adsorption isotherm. The Langmuir adsorption isotherm is a plot of C/θ vs C as represented in Fig. 2.

Adsorption of inhibitor molecules on the LCS surface by the Langmuir adsorption isotherm is provided by using the following equations:

$$\frac{C}{\theta} = \frac{1}{K_{\text{ads}}} + C \quad (5)$$

$$\theta = \frac{\text{IE}(\%)}{100} \quad (6)$$

where K_{ads} is the equilibrium adsorption constant, C is the inhibitor concentration and θ is the surface coverage.

The slope and regression coefficient (R^2) are near to 1 (Fig. 2), which indicates strong adsorption and formation of a monolayer coating on the LCS surface. Considering our previous investigation, *Myristica fragrans* shows K_{ads} (9.95 Lg^{-1}) with 83.27% IE at 500 mg/L, while in the present study the higher value of K_{ads} (16.12 Lg^{-1}) indicates better adsorption of the inhibitor molecule on the LCS surface with 90.63% IE at 600 mg/L.

3.2 UV-Visible Spectroscopy Analysis

To verify the adsorption phenomenon, UV-Visible spectroscopy technique has been used. UV-Vis analysis has been done in two modes, before and after the corrosion test.

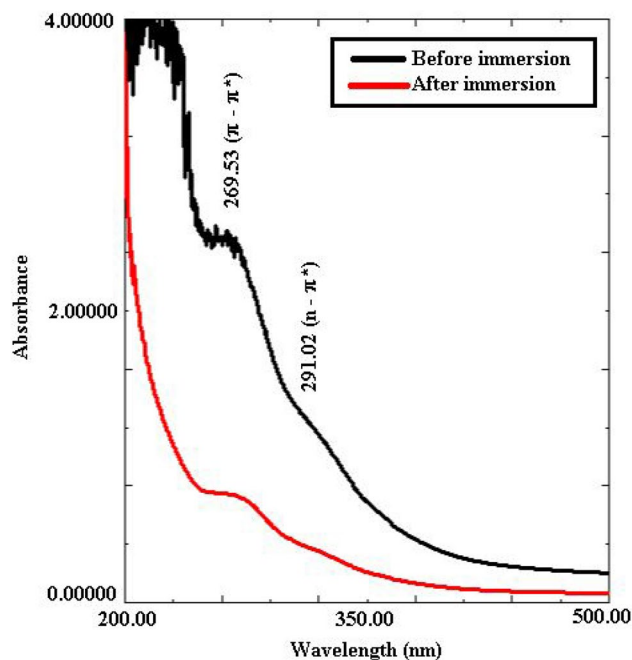


Fig. 3 UV-Vis. spectra of *E. globulus* extract after and before the corrosion test

Figure 3 shows the UV-Vis spectra of inhibitor. In this figure, two spectra have been shown one for UV-Vis spectra before the corrosion test and the second one is after the corrosion test. Before the corrosion test, inhibitor shows two adsorption peaks at 269.53 nm and 291.02 nm. These peaks can be assigned as $\pi-\pi^*$ and $n-\pi^*$ transitions. With the help of Fig. 3, we conclude that the graph shows a low adsorption peak after the corrosion test. In the comparison between both the spectra, a significant change has been found in the adsorption band because of the inhibitor molecules get adsorbed on the LCS surface [37].

3.3 FT-IR and ^1H NMR Studies

Fourier-transform infrared (FT-IR) spectroscopy technique has been carried out to investigate the presence of the various functional groups present in the phytochemical compounds. Figure 4 indicates the FT-IR spectrum of the pure leaf's extract of *E. globulus*. It was observed that the peak at 3382.36 cm^{-1} is due to O-H stretching of alcohol. The further peak at 2932.54 cm^{-1} due to the C-H stretching and the peak at 1071.98 cm^{-1} indicate C-O stretching.

For a deeper study of the adsorption phenomenon, ^1H NMR of the pure extract was carried out: ^1H NMR (CDCl_3 , 400 MHz/ppm), $\delta = 5.36$ (–OH, phenolic), $\delta = 7.28$ (– CH_2 , aromatic), $\delta = 3.68$ (–O– CH_2) and $\delta = 1.27$ (– CH_3). The presence of almost all the characteristic peaks is similar to the previously reported results [33, 34], which suggested the presence of reported major phytochemical constituents

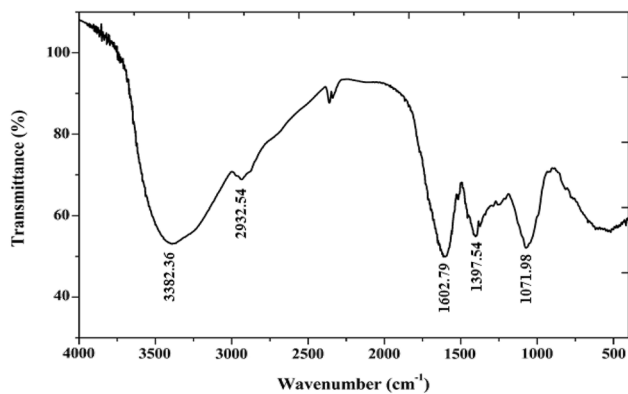


Fig. 4 FT-IR spectra of pure *E. globulus* leave's extract

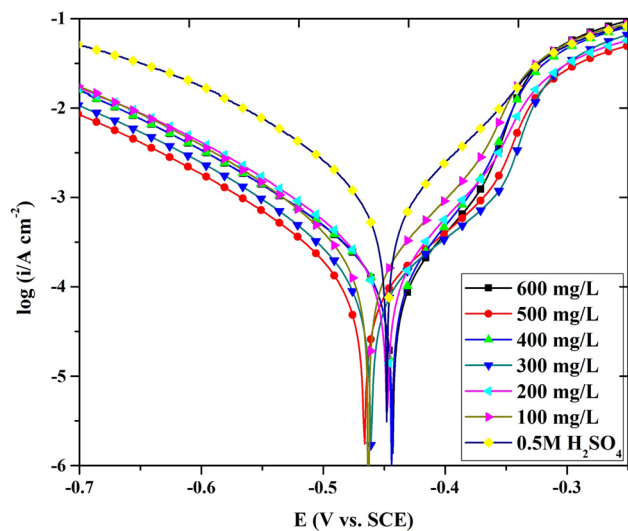


Fig. 5 Polarization curves of *E. globulus* on LCS in 0.5 M H₂SO₄ for a concentration range of 0–600 mg/L extract at 298 K

in the *E. globulus* extract. The phytochemicals containing heteroatoms and unsaturation has the polar function, so can be adsorbed on the metal surface as a protective layer. The adsorption of the polar atoms on the surface of the metal

may occur through coordination between the lone pair or π -electron cloud and the metallic surface [38].

3.4 Potentiodynamic Polarization Measurements

The concentration effect of the *E. globulus* extract on the polarization character for LCS in 0.5 M H₂SO₄ at 298 K was analysed. The Tafel plots were recorded at different inhibitor concentration, which is represented in Fig. 5.

Surface coverage values increase with increasing inhibitor concentration. From Tafel plots, we got the values of the anodic and cathodic Tafel slopes (β_a and β_c), corrosion current density (i_{corr}), corrosion potential (E_{corr}) and corrosion restraint effectiveness (IE %) with the help of the following equation [39]:

$$IE(\%) = \frac{i_{corr}^o - i_{corr}^i}{i_{corr}^o} \times 100 \tag{7}$$

where i_{corr}^i and i_{corr}^o represent the corrosion current density values with and without inhibitor, respectively. With the increase in inhibitor concentration, the polarization resistance (R_p) increases. These polarization resistance values were calculated from the slope of the potential–current plot,

$$\text{Linear polarization resistance (LPR)} R_p = \frac{1}{i_{corr}} \times \frac{\beta_a \times \beta_c}{2.303(\beta_a + \beta_c)} \tag{8}$$

where β_c and β_a are the cathodic and anodic Tafel slopes and i_{corr} is the corrosion current density.

Table 3 shows the polarization parameters for LCS in 0.5 M H₂SO₄ without and with different concentrations of *E. globulus* extract at 298 K. As per Fig. 5, each anodic metal dissolution and cathodic hydrogen development response were inhibited, once the inhibitors were added to the corrosive medium. The values of E_{corr} are within 85 mV with respect to the blank, which suggests that the studied inhibitor acts as a mixed type of corrosion inhibitor [40]. It should be noted that the addition of each concentration causes a remarkable decrease in anodic (β_a) and cathodic (β_c) Tafel

Table 3 Polarization parameters for LCS in 0.5 M H₂SO₄ without and with different concentrations of *E. globulus* at 298 K

Inhibitor concentration (mg/L)	$-E_{corr}$ (mV vs. SCE)	i_{corr} ($\mu\text{A cm}^{-2}$)	β_a (mV/dec)	$-\beta_c$ (mV/dec)	R_p ($\Omega \text{ cm}^2$)	Efficiency (IE %)	θ
0	465 ± 0.3	890.90 ± 1.3	141.66 ± 2.2	164.26 ± 2.1	37.07 ± 1.3	–	–
100	463 ± 0.5	136.50 ± 1.2	47.45 ± 2.1	108.30 ± 2.1	104.96 ± 2.1	84.67	0.8467
200	448 ± 0.2	124.90 ± 1.9	46.22 ± 1.7	111.19 ± 2.3	113.50 ± 1.7	85.98	0.8598
300	461 ± 0.7	100.40 ± 2.1	69.50 ± 1.3	109.30 ± 1.5	132.28 ± 1.2	88.73	0.8873
400	444 ± 0.6	91.80 ± 2.3	36.99 ± 2.3	114.62 ± 1.3	143.43 ± 1.6	89.70	0.8970
500	466 ± 0.5	88.30 ± 1.1	65.78 ± 1.9	112.68 ± 1.9	183.74 ± 1.9	90.08	0.9008
600	443 ± 0.4	76.60 ± 1.2	32.54 ± 1.3	113.75 ± 2.0	204.24 ± 2.3	91.40	0.9140

slopes. But the higher variation in anodic Tafel slopes (β_a) as compared to cathodic Tafel slopes (β_c) indicates its anodic way of reaction. The values in Table 3 depict that, with the increase in *E. globulus* concentration, the corrosion current density decreases. It is already known that the adsorptive inhibitors hinder the release of hydrogen gas on the LCS surface and/or reduce the dissolution process of LCS into the aggressive solution by blocking the active sites on LCS surface or even can mechanically screen the covered part of the electrode and therefore protect it from the action of acid solution. Following this way, the inhibition efficiency is expected to increase with the increase in inhibitor concentration. As per our previous investigation, the *M. fragrans* reports the value of i_{corr} ($112.00 \mu A cm^{-2}$) with 87.42% IE at 500 mg/L, while in the present study, the lowest value of i_{corr} ($76.60 \mu A cm^{-2}$) indicates a better corrosion inhibition with 91.40% IE at 600 mg/L.

3.5 Electrochemical Impedance Spectroscopy (EIS) Measurements

EIS measurements were performed to study the impedance parameters of LCS in 0.5 M H_2SO_4 at various concentrations of *E. globulus* at 298 K. Before each test, the working electrode was immersed in the test solution for 1 h at 298 K to attain the steady-state potential. It is clear from Fig. 6 that E_{OCP} remains almost constant after 1 h of immersion, which indicates a steady state. The temperature is maintained constant (298 K) for all the tests. To analyse the impedance parameters from the experimental outcomes, the data were fitted to the electrical equivalent circuit. Figure 7a shows the used electrical equivalent circuit in the appearance and nonappearance of the inhibitor. In the equivalent circuit, R_s

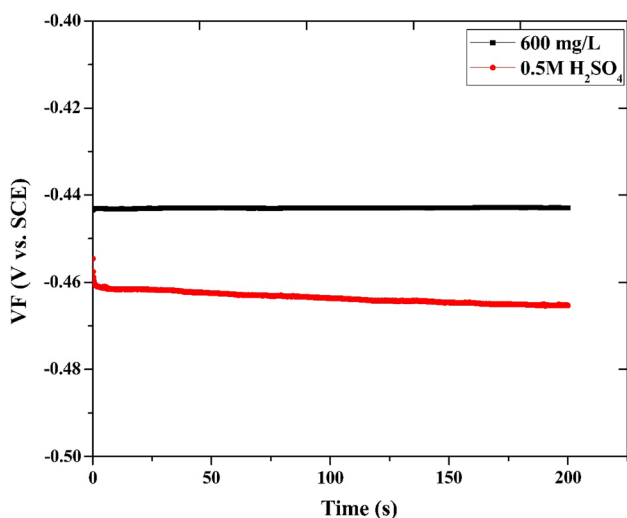


Fig. 6 OCP versus time curves for LCS in 0.5 M H_2SO_4 solution in absence and presence of 600 mg/L *E. globulus* extract at 298 K

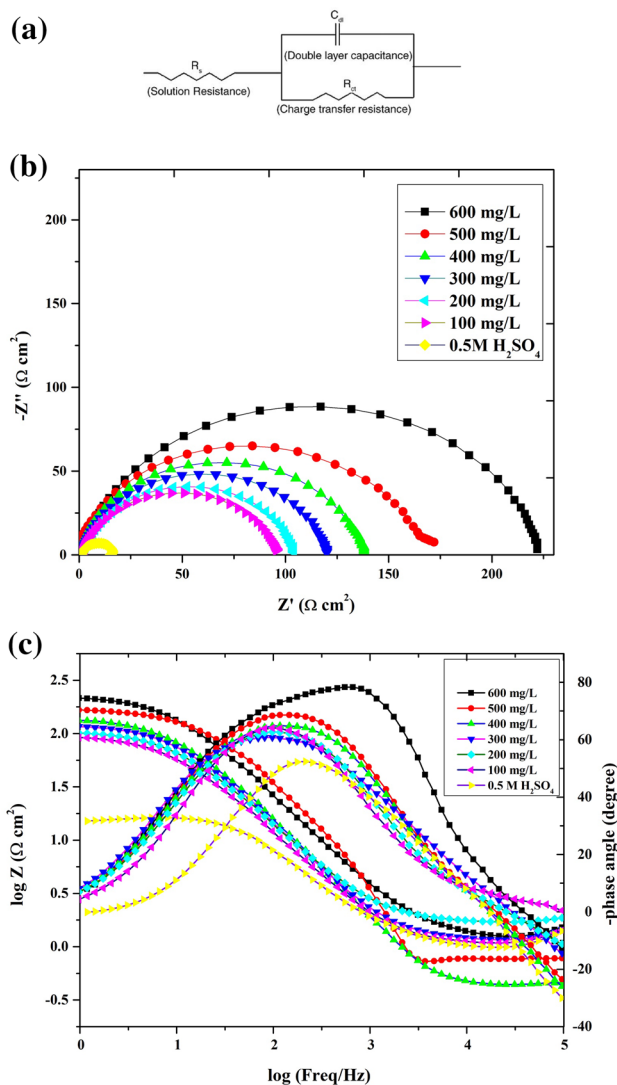


Fig. 7 a Equivalent circuit, b Nyquist, and Bode, and c plots of LCS in 0.5 M H_2SO_4 solution in the absence and the presence of *E. globulus* extract

is the solution resistance, R_{ct} is the charge exchange resistance, and C_{dl} is the double-layer capacitance. The results are reported in Table 4.

The EIS curves (Nyquist and Bode plots) for LCS with and without *E. globulus* extract are shown in Fig. 7b, c. The inhibition efficiency based on impedance study can be calculated by using the following equation:

$$IE(\%) = \frac{R_{ct} - R_{ct}^0}{R_{ct}} \times 100 \tag{9}$$

where R_{ct} and R_{ct}^0 are the charge transfer resistance with and without the inhibitor, respectively.

As evident from Table 4, the values of C_{dl} have decreased and R_{ct} have increased by the increase in

Table 4 EIS parameters of LCS in 0.5 M H₂SO₄ without and at different concentrations of *E. globulus* at 298 K

Concentration of inhibitor (mg/L)	R_{ct} (Ω cm ²)	f_{max} (Hz)	R_s (Ω cm ²)	C_{dl} (μ F cm ⁻²)	n	Efficiency (IE %)	θ
0	15.71 ± 1.3	37.60 ± 0.5	1.22 ± 0.1	269.49 ± 1.2	0.57 ± 0.01	–	–
100	98.07 ± 1.1	6.64 ± 0.3	1.28 ± 0.1	244.00 ± 1.3	0.79 ± 0.03	83.98	0.8398
200	105.46 ± 1.3	8.07 ± 0.2	1.83 ± 0.3	187.00 ± 1.7	0.83 ± 0.05	85.10	0.8510
300	121.11 ± 1.7	8.07 ± 0.2	1.33 ± 0.7	168.00 ± 1.1	0.86 ± 0.03	87.02	0.8702
400	142.12 ± 1.9	6.64 ± 0.3	0.45 ± 0.5	162.00 ± 1.0	0.88 ± 0.04	88.94	0.8894
500	174.84 ± 2.1	6.64 ± 0.5	0.77 ± 0.4	137.00 ± 1.3	0.92 ± 0.04	91.01	0.9101
600	227.48 ± 3.1	5.49 ± 0.7	1.43 ± 0.6	127.00 ± 2.3	0.96 ± 0.07	93.09	0.9309

the inhibitor concentration. This may be attributed to the decreased in local dielectric constant and/or to the increase in the thickness of the C_{dl} . The dissolution mechanism could be predicted by the values of the phase shift (n) as an indicator. It is clear that a slight change in the value of n is observed after addition of various inhibitor concentrations. The almost invariable values of n indicate that the charge transfer process controls the dissolution mechanism in both the absence and the presence of various inhibitor concentrations. The inhibition efficiency was found to be improved with the increase in the concentration of *E. globulus* extract. The maximum inhibition efficiency was achieved at 600 mg/L inhibitor concentration. The molecules present in the plant extract can be adsorbed on the surface of the LCS by the mechanism of donating π -electrons of the aromatic rings or lone pair of electrons of the heteroatoms to the vacant orbital of iron [41–44]. These compounds can form a protective layer to protect the LCS surface from the corrosive medium. Although the graphs for the uninhibited and inhibited systems are similar, probably due to the similar mechanism of corrosion, the influence of the inhibit on the corrosion process is obvious. The effect, which is concentration-dependent, is manifested in the larger diameter of the capacitive loops, the displacement of the impedance and the phase angle to larger values in the extract-inhibited systems relative to the blank. This could be possible due to the obstruction of reaction points on the metal surface by adsorbed inhibitor molecules.

The results clearly demonstrate that *E. globulus* extract inhibits the corrosion of LCS at any concentration, and with the increase in the inhibitor concentration, inhibition effectiveness increases [45, 46]. As per our previous investigation, the *M. fragrans* reports the value of R_{ct} (128.88 Ω cm²) with 87.81% IE at 500 mg/L, while in the present study, the highest value of R_{ct} (227.48 Ω cm²) confirms the better corrosion inhibition with 93.09% IE at 600 mg/L.

3.6 Theoretical Studies

3.6.1 Quantum Chemical Calculations

Plant extracts have lots of phytochemical components. There are three main components of *E. globulus* selected for the theoretical study. *E. globulus* contains eucalyptol, globulisin-A and globulisin-B as the main phytochemical components. Figure 8 shows the optimized, HOMO and LUMO orbitals of the eucalyptol, globulisin-A and globulisin-B molecules. Following equations have been used to calculate different quantum chemical parameters [47]:

$$\Delta E = E_{LUMO} - E_{HOMO} \quad (10)$$

$$\eta = \frac{1}{2}(E_{LUMO} - E_{HOMO}) \quad (11)$$

$$\chi = -\frac{1}{2}(E_{LUMO} + E_{HOMO}) \quad (12)$$

$$\Delta N = \frac{\chi_{Fe} - \chi_{inh}}{2(\eta_{Fe} - \eta_{inh})} \quad (13)$$

$$\sigma = \frac{1}{\eta} \quad (14)$$

$$\Delta E_{Back\ Donation} = -\frac{\eta}{4} \quad (15)$$

$$\pi = -\chi \quad (16)$$

where χ_{inh} and χ_{Fe} demonstrate the electronegativity of inhibitor molecule and iron, respectively. η_{inh} and η_{Fe} means the hardness of the inhibitor molecule and iron, respectively. A value of 7 eV/mol has been taken for the χ_{Fe} , whereas a value of 0 eV/mol has been taken for η_{Fe} , as per the Pearson's electronegativity scale. η is the softness value of

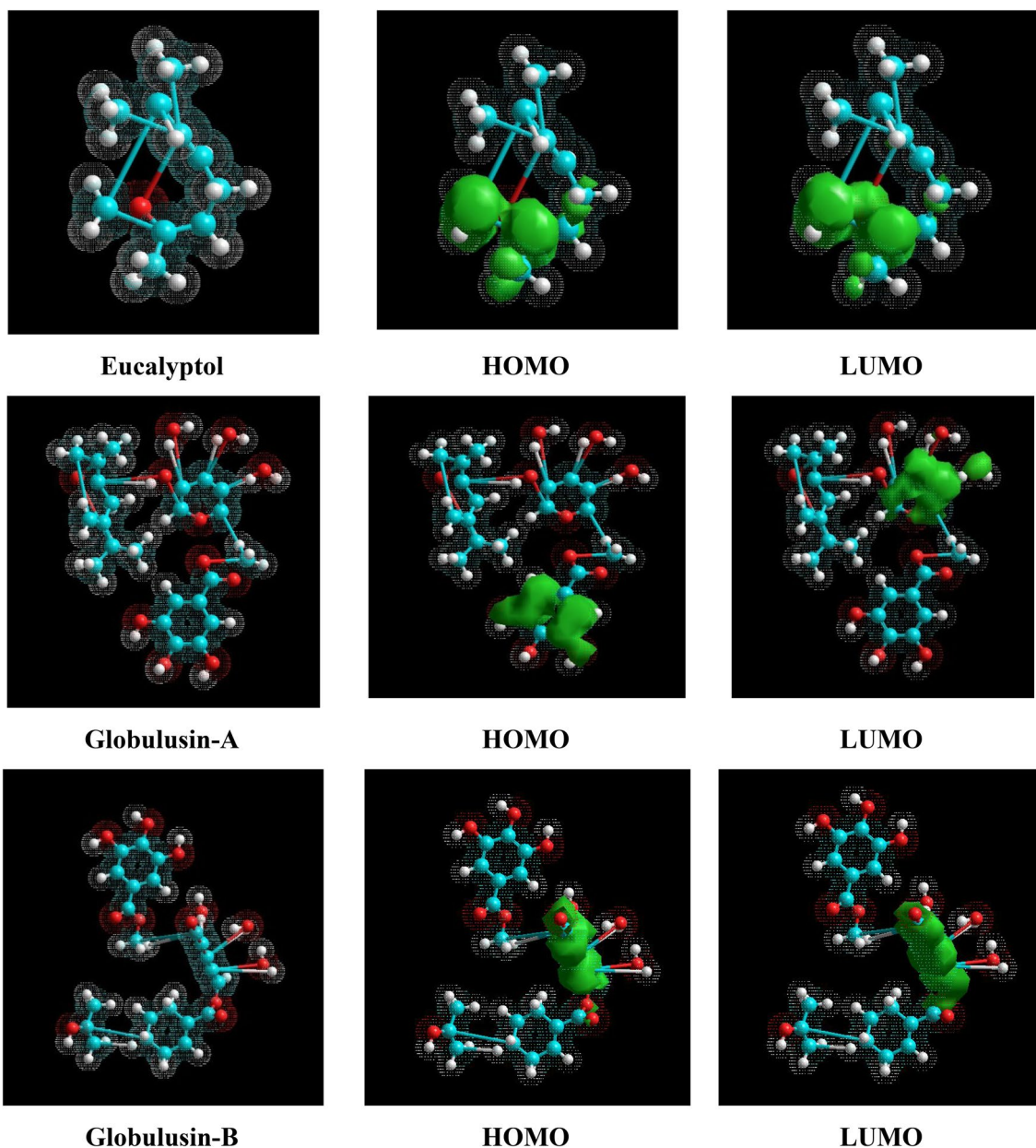


Fig. 8 Optimized structures and frontier molecular orbital density distributions (HOMO & LUMO) of eucalyptol, globulusin-A and globulusin-B molecules obtained by DFT/B3LYP/6-31G+(d, p) method

the inhibitor molecule and σ is the chemical hardness of the inhibitor molecule. $\Delta E_{\text{BackDonation}}$ (Eq. 18) intimates that, at $\eta > 0$ and $< \Delta E_{\text{BackDonation}} 0$, the charge transfer to a molecule, took after by a back-donation starting with the molecule, is favoured energetically, and π is the chemical potential.

As per Table 5, the high value of E_{HOMO} of eucalyptol (0.93 eV) indicates that the eucalyptol molecule has a fundamentally high affinity of charge donation to the LCS surface. Globulusin-B has the least E_{LUMO} (−0.41 eV), which shows the highest ability to accept electrons from the d -orbital of Fe. Globulusin-A has the lowest value of ΔE (0.01 eV),s

which shows its highest reliability of forming the [Fe-globulusin-A] complex. Moreover, eucalyptol has a rather high value of μ (1.42 D), which indicates strong adsorption of eucalyptol molecule on the LCS surface [48].

3.7 SEM and AFM Analysis

Figure 9 highlights scanning electron microscopy (SEM) and atomic force microscopy (AFM) micrographs of LCS surface prior and afterwards the corrosion tests without and with the inhibitor. Figure 9a shows the SEM and AFM

Table 5 Quantum chemical parameters calculated for the eucalyptol, globulisin-A and gslobulisin-B molecules by the method DFT/B3LYP/6-31G+(d, p)

Molecule	E_{HOMO} (eV)	E_{LUMO} (eV)	ΔE (eV)	μ (D)	ΔN (e)	$\Delta E_{\text{Back-Donation}}$ (eV)	η (eV)	σ (eV ⁻¹)	χ (eV)	π (eV)
Eucalyptol	0.93	1.75	0.81	1.42	10.23	-0.10	0.41	2.45	-1.34	1.34
Globulisin-A	0.86	0.85	0.01	0.38	142.6	-0.01	0.01	36.36	-0.86	0.86
Globulisin-B	-0.41	-0.27	0.14	1.17	47.30	-0.02	0.07	14.20	0.34	-0.34

micrographs of abraded LCS surface. It shows a sleek surface with least surface roughness (2.99 nm) and maximum height (60 nm) values. Figure 9b shows the LCS surface after the corrosion test without the inhibitor. In this case, the LCS surface is highly corroded due to the acidic corrosive media, resulting in a rough micrograph with highest surface roughness (138.81 nm) and maximum height (2100 nm) values obtained. Figure 9c shows the LCS surface after the corrosion test with the inhibitor (600 mg/L). It shows the presence of the inhibitor covers the surface and prevents the corrosion process with much lower surface roughness (26.86 nm) and maximum height (300 nm) values. It is very less than the outcomes obtained in the case of without inhibitor. The decrease in height and average surface roughness of the LCS specimen is due to the adsorption of *E. globulus* inhibitor on the metal surface. It can be said that a protective layer is formed on the surface of the metal. It verifies *E. globulus* adsorb on the surface of the LCS creating a protective layer to prevent the corrosion process on the LCS surface.

3.8 The Proposed Mechanism of Action

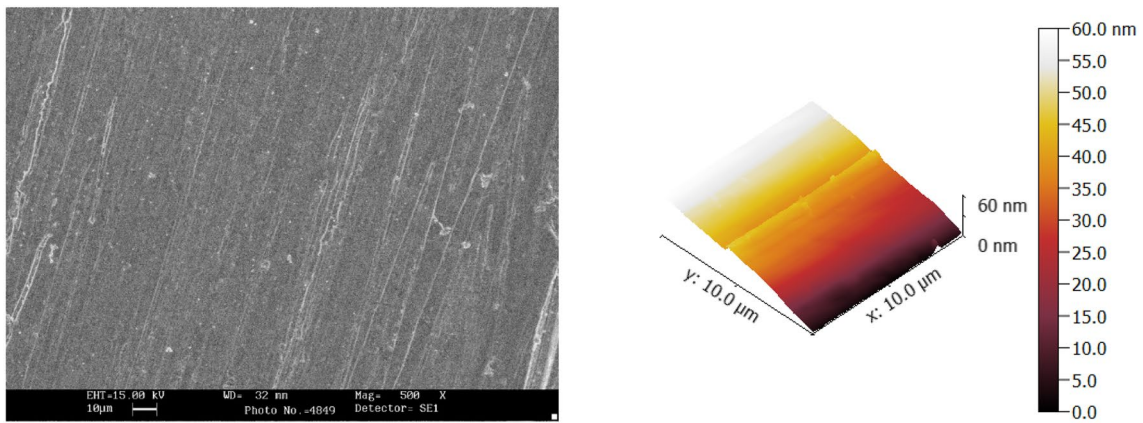
To explain the inhibitory effect of *E. globulus* on LCS in 0.5 M H₂SO₄, it is important to evaluate the experimental and calculated results and correlate them with the structural, chemical and electronic properties of the inhibitory molecules. *E. globulus* contains several phytochemical compounds having a number of heteroatoms and aromatic rings. These compounds act as Lewis bases and form coordination bonds with the free *d*-orbital of Fe and adsorb on a LCS surface to form a protective layer on the LCS surface to protect against corrosive environments. The HOMO orbitals of the molecules studied indicate that a uniform pair of electrons are available for nucleophilic interaction (chemisorption) with the LCS surface. The LUMO in the heteroatoms causes the formation of $d\pi-d\pi$ bonds, and the formation of superimposed three-dimensional electrons of iron atoms with a free spatial

orbital heteroatom is possible. Also, the adsorption can be done by electrostatic interaction (physisorption) between heteroatoms and the Fe²⁺. Retro-donation can be done using π -electrons of aromatic rings. This phenomenon is also verified by theoretical studies and polarization measurements. Figure 10 shows the proposed mechanism for the adsorption phenomenon of globulisin B molecule adsorbed on a LCS surface.

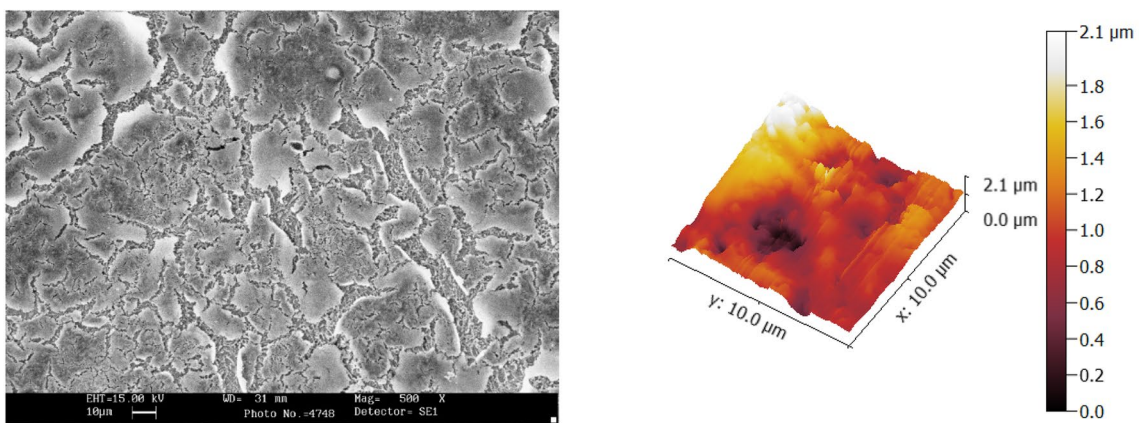
4 Conclusion

The inhibition effect and adsorption behaviour of the leaves extract of *E. globulus* have been investigated using weight loss measurements, electrochemical studies, SEM and AFM surface investigations, FT-IR, ¹H NMR and quantum chemical calculations. The conclusions of these investigations are as follows:

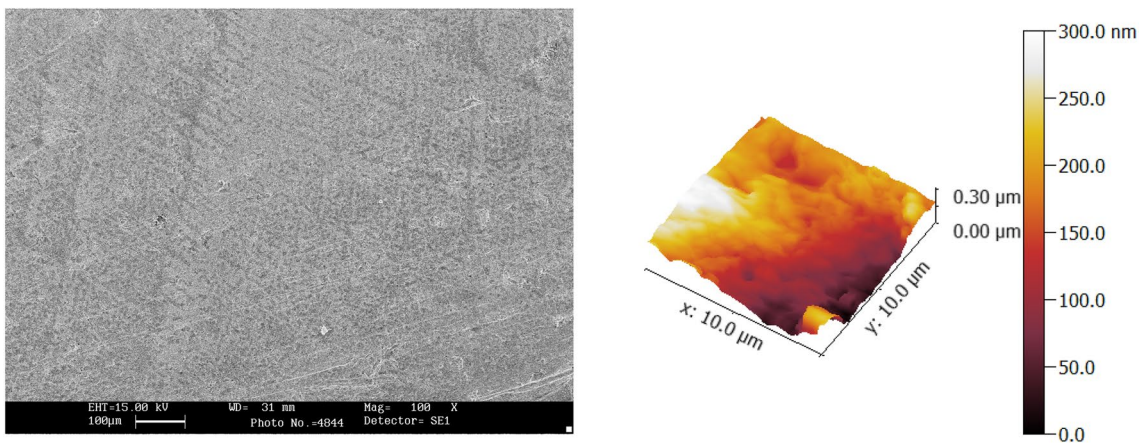
- *E. globulus* leave's extract was investigated as a sustainable and green corrosion inhibitor for LCS in 0.5 M H₂SO₄.
- The gravimetric estimations and the electrochemical studies confirmed that the inhibition efficiency of *E. globulus* extract is > 93% at 600 mg/L.
- Verification of various functional groups containing heteroatoms and unsaturation in the phytochemical constituents of the plant extract was done by using FT-IR and ¹H NMR techniques.
- UV-Visible technique verified the formation of coordination bonds between inhibitor molecules and Fe²⁺.
- The prime phytochemical constituents were simulated using density functional theory (DFT) and the results support the experimental outcomes.
- The surface adsorption of *E. globulus* extract was investigated by using scanning electron microscopy (SEM) supported by atomic force microscopy (AFM) technique.



(a) Abrade steel



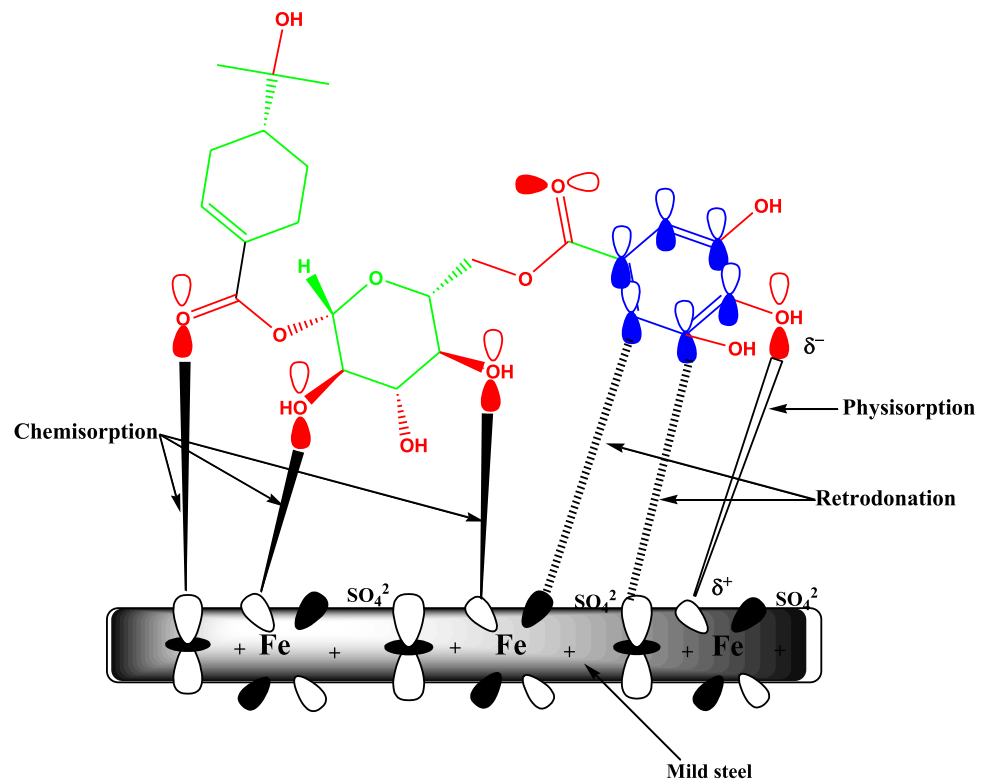
(b) Without inhibitor



(c) With inhibitor

Fig. 9 AFM and SEM micrographs of the surface of mild steel after 24 h immersion at 298 K in 0.5 M H_2SO_4 **a** abrade steel, **b** without inhibitor and **c** with inhibitor (600 mg/L)

Fig. 10 Suggested mechanism of adsorption behaviour of the globulisin-B molecule on LCS surface



Acknowledgements We are thankful to Prof. Gurmeet Singh, Department of Chemistry, University of Delhi, Delhi-110007, INDIA, for providing the lab facility for the research work.

Compliance with Ethical Standards

Conflict of interest The authors declared that they have no conflicts of interest.

References

- Amin MA, Abd El-Rehim SS, El-Sherbini EEF, Bayoumi RS (2007) The inhibition of low carbon steel corrosion in hydrochloric acid solutions by succinic acid. Part I. Gravimetric measurements, polarization, EIS, PZC, EDX and SEM studies. *Electrochim Acta* 52:3588–3600
- Koch G (2015) *Trands in oil and gas corrosion research and technologies*. Woodhead Publishing, Cambridge
- Ahamad I, Prasad R, Quraishi MA (2010) Experimental and quantum chemical characterization of the adsorption of some Schiff base compounds of phthaloyl thiocarbonylhydrazide on the mild steel in acid solutions. *Mater Chem Phys* 124:1155–1165
- Abd El-Lateef HM, Abo-Riya MA, Tantawy AH (2016) Empirical and quantum chemical studies on the corrosion inhibition performance of some novel synthesized cationic gemini surfactants on carbon steel pipelines in acid pickling processes. *Corros Sci* 108:94–110
- Bagga MK, Gadi R, Yadav OS, Kumar R, Chopra R, Singh G (2016) Investigation of phytochemical components and corrosion inhibition property of *Ficus racemosa* stem extract on mild steel in H₂SO₄ medium. *J Environ Chem Eng* 4:4699–4707
- Hassan KH, Khadom AA, Kurshed NH (2016) *Citrus aurantium* leaves extracts as a sustainable corrosion inhibitor of mild steel in sulfuric acid. *S Afr J Chem Eng* 22:1–5
- Patel N, Rawat A, Jauhari S, Mehta G (2010) Inhibitive action on *Bridelia restusa* leaves extract on corrosion of mild steel in acidic media. *Eur J Chem* 1:129–133
- Ibrahim T, Alayan H, Al Mowaqet Y (2012) The effect of Thyme leaves extract on corrosion of mild steel in HCl. *Prog Org Coatings* 75:456–462
- Al-Otaibi MS et al (2013) The effect of temperature on the corrosion inhibition of mild steel in 1 M HCL solution by *Curcuma longa* extract. *Int J Electrochem Sci* 5:847–859
- Vasudha VG, Shanmuga Priya K (2013) *Polyalthia longifolia* as a corrosion inhibitor for mild steel in HCl solution. *Res J Chem Sci* 3:21–26
- Garai S, Garai S, Jaisankar P, Singh JK, Elango A (2012) A comprehensive study on crude methanolic extract of *Artemisia pallens* (Asteraceae) and its active component as effective corrosion inhibitors of mild steel in acid solution. *Corros Sci* 60:193–204
- Rose K, Kim BS, Rajagopal K, Arumugam S, Devarayan K (2016) Surface protection of steel in acid medium by *Tabernaemontana divaricata* extract: Physicochemical evidence for adsorption of inhibitor. *J Mol Liq* 214:111–116
- Oguzie EE, Chidiebere MA, Oguzie KL, Adindu CB, Momoh-Yahaya H (2014) BioLC-MS extracts for materials protection: Corrosion inhibition of mild steel in acidic media by *Terminalia chebula* extracts. *Chem Eng Commun* 201:790–803
- Haldhar R, Prasad D, Saxena A, Singh P (2018) *Valeriana wallichii* root extract as a green & sustainable corrosion inhibitor for mild steel in acidic environments: experimental and theoretical study. *Mater Chem Front* 2:1225–1237
- Saxena A, Prasad D, Haldhar R (2018) Use of *Asparagus racemosus* extract as green corrosion inhibitor for mild steel in 0.5 M H₂SO₄. *J Mater Sci* 53:8523–8535

16. Saxena A, Prasad D, Haldhar R (2016) *Withania somnifera* extract as green inhibitor for mild steel in 8 % H₂SO₄. Asian J Chem 28:2471–2474
17. Soltani N, Tavakkoli N, Khayat Kashani M, Jalali MR, Mosavizade A (2012) Green approach to corrosion inhibition of 304 stainless steel in hydrochloric acid solution by the extract of *Salvia officinalis* leaves. Corros Sci 62:122–135
18. Haldhar R, Prasad D, Saxena A (2018) *Myristica fragrans* extract as an eco-friendly corrosion inhibitor for mild steel in 0.5 M H₂SO₄. J Environ Chem Eng 6:2290–2301
19. Rahim A, Rocca E, Steinmetz J, Kassim M, Adnan R, Sani Ibrahim M (2007) *Mangrove tannins* and their flavanoid monomers as alternative steel corrosion inhibitors in acidic medium. Corros Sci 49:402–417
20. Deng S, Li X (2012) Inhibition by *Jasminum nudiflorum* Lindl. leaves extract of the corrosion of aluminium in HCl solution. Corros Sci 64:253–262
21. Ostovari A, Hoseinie SM, Peikari M, Shadizadeh SR, Hashemi SJ (2009) Corrosion inhibition of mild steel in 1 M HCl solution by henna extract: A comparative study of the inhibition by henna and its constituents (Lawson, Gallic acid, alpha-D-Glucose and Tannic acid). Corros Sci 51:1935–1949
22. Li X, Deng S (2012) Inhibition effect of *Dendrocalamus brandisii* leaves extract on aluminum in HCl, H₃PO₄ solutions. Corros Sci 65:299–308
23. Torres VV, Amado RS, Sa CF, Fernandez TL, Riehl CAS, Torres AG, D'Elia E (2011) Inhibitory action of aqueous coffee ground extracts on the corrosion of carbon steel in HCl solution. Corros Sci 53:2385–2392
24. Okafor PC, Ikpi ME, Uwah IE, Ebenso EE, Ekpe UJ, Umoren SA (2008) Inhibitory action of *Phyllanthus amarus* extracts on the corrosion of mild steel in acidic media. Corros Sci 50:2310–2317
25. Radojčić I, Berković K, Kovač S, Vorkapić-Furač J (2008) Natural honey and black radish juice as tin corrosion inhibitors. Corros Sci 50:1498–1504
26. Deng S, Li X (2012) Inhibition by Ginkgo leaves extract of the corrosion of steel in HCl and H₂SO₄ solutions. Corros Sci 55:407–415
27. Njoku DI, Ukaga I, Ikenna OB, Oguzie EE, Oguzie KL, Ibisí N (2016) Natural products for materials protection: Corrosion protection of aluminium in hydrochloric acid by *Kola nitida* extract. J Mol Liq 219:417–424
28. Noor EA (2011) The impact of some factors on the inhibitory action of Radish fruits aqueous extract for mild steel corrosion in 1 M H₂SO₄ solution. Mater Chem Phys 131:160–169
29. Haldhar R, Prasad D, Bhardwaj N (2020) Surface adsorption and corrosion resistance performance of *Acacia concinna* pod extract: An efficient inhibitor for mild steel in acidic environment. Arab J Sci Eng 45:131–141
30. Li X, Deng S, Fu H (2012) Inhibition of the corrosion of steel in HCl, H₂SO₄ solutions by bamboo leaf extract. Corros Sci 62:163–175
31. Joseph O, Favomi O, Adenigba O (2017) Effect of *Lecaniodiscus cupanioides* extract in corrosion inhibition of normalized and annealed mild steels in 0.5 M HCl. Energy Proc 119:845–851
32. Azzoui K, Mejdoubi E, Jodeh S (2017) Eco friendly green inhibitor *Gum arabic* (GA) for the corrosion control of mild steel in hydrochloric acid medium. Corros Sci 129:70–81
33. Maciel MV et al (2010) Chemical composition of *Eucalyptus spp.* essential oils and their insecticidal effects on *Lutzomyia longipalpis*. Phytochemistry 167:1–7
34. Hasegawa T, Takano F, Takata T, Niiyama M, Ohta T (2008) Bioactive monoterpene glycosides conjugated with gallic acid from the leaves of *Eucalyptus globulus*. Phytochemistry 69:747–753
35. Saxena A, Prasad D, Haldhar R, Singh G, Kumar A (2018) Use of *Saraca ashoka* extract as green corrosion inhibitor for mild steel in 0.5 M H₂SO₄. J Mol Liq 258:89–97
36. Verma C, Quraishi MA, Ebenso EE, Obot IB, El Assry A (2016) 3-Amino alkylated indoles as corrosion inhibitors for mild steel in 1M HCl: Experimental and theoretical studies. J Mol Liq 219:647–660
37. Saxena A, Prasad D, Haldhar R, Singh G, Kumar A (2018) Use of *Sida cordifolia* extract as green corrosion inhibitor for mild steel in 0.5 M H₂SO₄. J Environ Chem Eng 6:694–700
38. Kumar R, Yadav OS, Singh G (2017) Electrochemical and surface characterization of a new eco-friendly corrosion inhibitor for mild steel in acidic media: a cumulative study. J Mol Liq 237:413–427
39. Ahamad I, Quraishi MA (2010) Mebendazole: New and efficient corrosion inhibitor for mild steel in acid medium. Corros Sci 52:651–656
40. Daoud D, Douadi T, Hamani H, Chafaa S, Al-Noaimi M (2015) Corrosion inhibition of mild steel by two new S-heterocyclic compounds in 1 M HCl: Experimental and computational study. Corros Sci 94:21–37
41. Haldhar R, Prasad D, Saxena A, Kumar R (2018) Experimental and theoretical studies of *Ficus religiosa* as green corrosion inhibitor for mild steel in 0.5 M H₂SO₄ solution. Sustain Chem Pharm 9:95–105
42. Bhardwaj N, Prasad D, Haldhar R (2018) Study of *Aegle marmelos* as a green corrosion inhibitor for mild steel in acidic medium: Experimental and theoretical approach. J Bio-Tribo-Corros 4:1–10
43. Ashassi-Sorkhabi H, Asghari E (2008) Effect of hydrodynamic conditions on the inhibition performance of l-methionine as a 'green' inhibitor. Electrochim Acta 54:162–167
44. Zheng X, Zhang S, Li W, Yin L, He J, Wu J (2014) Investigation of 1-butyl-3-methyl-1H-benzimidazolium iodide as inhibitor for mild steel in sulfuric acid solution. Corros Sci 80:383–392
45. Mahdavian M, Attar MM (2009) Electrochemical behaviour of some transition metal acetylacetonate complexes as corrosion inhibitors for mild steel. Corros Sci 51:409–414
46. Hejazi S et al (2015) Electrochemical and quantum chemical study of Thiazolo-pyrimidine derivatives as corrosion inhibitors on mild steel in 1M H₂SO₄. J Ind Eng Chem 25:112–121
47. Salarvand Z, Amirnasr M, Talebian M, Raeissi K, Meghdadi S (2017) Enhanced corrosion resistance of mild steel in 1M HCl solution by trace amount of 2-phenyl-benzothiazole derivatives: Experimental, quantum chemical calculations and molecular dynamics (MD) simulation studies. Corros Sci 114:133–145
48. Morad MS (2000) An electrochemical study on the inhibiting action of some organic phosphonium compounds on the corrosion of mild steel in aerated acid solutions. Corros Sci 42:1307–1326

Publisher's Note Springer Nature remains neutral with regard to jurisdictional claims in published maps and institutional affiliations.